OPEN ACCESS

University of BRISTOL

Courtier, M., Croxford, A., & Atherton, K. (2016). Guided Wave Propagation Modelling to Aid Understanding of Acoustic Emission System Performance on Complex Aerospace Structures. The e-Journal of Nondestructive Testing & Ultrasonics.

Peer reviewed version

Link to publication record in Explore Bristol Research
PDF-document

## University of Bristol - Explore Bristol Research
### General rights

# Guided Wave Propagation Modelling to Aid Understanding of Acoustic Emission System Performance on Complex Aerospace Structures

Mark R. COURTIER [1], Anthony J. CROXFORD [1], Kathryn ATHERTON [2]

[1] Dpt Mechanical Engineering, University of Bristol, Queen's Building, University Walk, Bristol, BS8 1TR, UK      m.r.courtier@bristol.ac.uk
[2] Airbus Operations Ltd, Filton, Bristol, BS34 7PA, UK

## Abstract

*The design of acoustic emission structural health monitoring systems often only considers the plate properties of a structure and not the features present. Here a practical modelling approach is demonstrated to aid the understanding of how wave propagation within a structure affects the performance of an acoustic emission system. Empirical models of a row of 5 mm holes and a bolted L-section, a common feature in aerospace structures, are found from experimental results and incorporated in the system model. The model is used to assess which transducers acoustic emission events at different positions will trigger and how the position of transducers and the number of transducers used will affect event location error. This demonstrates potential uses of the modelling.*

## 1 INTRODUCTION

Acoustic Emission (AE) systems have been proposed to monitor damage growth in aircraft structure both in service and during development, for example to monitor structural tests. In an AE system a sparse array of ultrasonic transducers is bonded to the structure to be monitored. As damage occurs, energy is released by fracture and this is dissipated in the structure as heat and vibration. In the thin and plate like structure considered here, the vibration is converted into guided ultrasonic Lamb waves which can propagate large distances. This allows a reasonably large spacing between the transducers of approximately 1 m which is necessary in an aerospace application to limit the added weight of the system. Reception of the guided waves by a transducer enables damage growth to be detected and if the guided waves are received on 3 or more transducers then the source of the AE can be localised. This enables an AE system to monitor damage growth in a structure over a large area.

A known challenge when implementing AE systems is that the system performance decreases as the complexity of the structure increases [1, 2]. This is because thickness changes, holes, fasteners, stiffeners and many other kinds of structural feature cause reflections, velocity changes and mode conversions of the guided waves. This has the effect of increasing the attenuation of first arrival from the AE event, which is typically the section of the wave used for detection and location, and this attenuation is dependant on direction and location. This causes two

challenges; the attenuation of the wave is higher than predicted by the traditional assumption of a plate like structure and the time of flights for the AE events are different to what is expected by most location algorithms which assume a constant velocity profile [3, 4]. Location algorithms which can incorporate a changing velocity profile across the structure do exist but require significant effort to implement [5, 6].

The negative affects of the structure on the performance of AE systems has been noted by previous work including [7, 8]. Hamstad [7] highlights that these affects are rarely considered explicitly in industrial AE testing and it is the authors experience that this is still the case today. To a certain extent, compensation for greater feature density is often done intuitively by increasing the number of transducers in these regions. By modelling the affects of the structure it is hoped that they can be understood more rigorously which will benefit future system design and interpreting results from current systems.

## 2    MODELLING APPROACH

One possible approach would be to use Finite Element (FE) modelling to predict the guided wave propagation through the structure. This approach has been discounted here because FE models of guided waves require a small element size with greater than 10 elements per wavelength. For the size of structures considered here, of multiple metres in length and width, this requires an extremely large amount of computational time. To repeat this for multiple AE events at different locations throughout the structure is considered unfeasible.

The approach used here is the Linear Time-Invariant (LTI) systems approach. This is the same approach as used by Scholey in [9]. Each component of an AE system is modelled in the frequency domain for relevant ray paths. This modelling approach has been chosen because it is significantly less computationally intensive than FE and can model the relevant affects on the first arrival part of the signal. This part of the signal is traditionally the section processed by AE systems. Using this technique it is computationally feasible to model system performance from many AE events across the structure.

For the direct ray path from the AE source to each transducer in the array for the fastest mode the received signal spectrum, $H(\omega)$, is calculated using the following equation:

$$H(\omega) = S_E(\omega)U(\omega)R_x(\omega)P(\omega)A(\omega)B \prod_{1:n} T_C(\omega) \tag{1}$$

Where:

$S_E(\omega)$  is the frequency spectrum of the source excited in the relevant material. The source model used here is based upon the results in [10] from a fatigue crack in a large aluminium plate. Due to the large size of the plate, the characterisation is free from the influences of the edges of the sample. The maximum amplitude of the $S_0$ source signal is 0.08 V. The remainder of the source characteristics are undefined by this paper so are set that the source is a 2 cycle, Hanning window tone burst which is centred at a frequency of 150 kHz. This is done to be consistent with [9]. The source is assumed to show no directionality because the material in which the waves are being excited, aluminium, is isotropic.

$U(\omega)$  is the amplifier transfer function. For simplicity this component has been discounted in the following results so $U(\omega) = 1$. It could be added in from a amplifier specification or an experimental characterisation of an amplifier.

2

$R_x(\omega)$ is the transfer function of the receiving transducer. A frequency independent scaling factor has been used so $R_x(\omega) = \zeta$.

$P(\omega)$ is the time delay due to propagation and is calculated by $P(\omega) = e^{-\frac{i\omega d}{c(\omega)}}$ where $d$ is the propagation distance and $c(\omega)$ is the frequency dependent phase velocity.

$A(\omega)$ is the attenuation. The structures considered here are aluminium where the attenuation is negligible so $A(\omega) = 1$. For composite structures an appropriate attenuation model could be included here.

$B$ is the beam spread where $B = \frac{1}{\sqrt{d}}$.

$T_C(\omega)$ is the transmission coefficient for the $n$th feature where there are $n$ features on the ray path. This is where the majority of the effort in this work has been expended and feature models will be discussed in section 3.

## 3 FEATURE MODELS

The propagation of ultrasonic guided waves across a variety of different structural features common in aerospace structures has been considered in the literature and will be summarised here. Much of this has been done with respect to direct inspection of bondlines with guided waves as this is a problem which is difficult to assess with traditional NDT methods. However many of the models are general to the transmission of guided waves for any application so could be included in above model.

A common and simple feature found in aircraft is a thickness change in a plate. It is clear that the two different thickness's will have different dispersion curves but the feature will also affect the wave propagation. Pagneux and Maurel [11] present an analytical model for a thickness change and Cho [12] models this numerically using a hybrid boundary element method and validates the results experimentally. Another feature commonly studied in the literature is the adhesively bonded lap joint. Methods to model this situation include analytical [13, 14] and finite element [15] techniques. All of these approaches are successfully validated with experimental results.

Multiple feature models therefore already exist and can be used within the modelling framework described in section 2. However Dalton *el al.* show in [16], that when multiple features are present, the attenuation can be prohibitive high for many frequencies of operation. However an example of successful detection of a defect on a moderately complex structure is shown in [17]. A composite plate with two stringers is monitored and, by considering the interaction of the stringers, arrivals from a delamination are identified. The transducer density however is sufficiently high that the affect of only one stringer needs to be considered. Ideally operation across multiple stringers or features would be possible. Work by Flynn *et al.* [2] shows that a significant improvement in detection can be achieved with a very simple model of a stringer. The promising results from that paper form the basis of this work.

## 4 TRANSMISSION ACROSS A L-SECTION

A feature not included in the literature above is a bolted L-section so the transmission across this will now be found experimentally. These results will be used to inform an empirical model of the feature. Features similar in shape to a L-section are common in aircraft structure as stiffeners and are therefore a relevant feature to model. The transmission across a smaller L-section of 25 mm in width and height is measured in [18] and is approximately 0.8 for the measured incident angles of 0° to 45°. A larger range of incident angles will be measured here
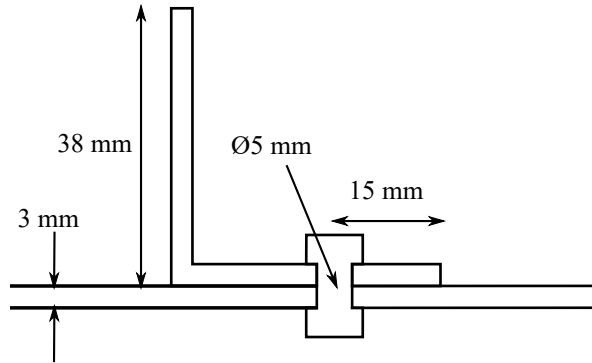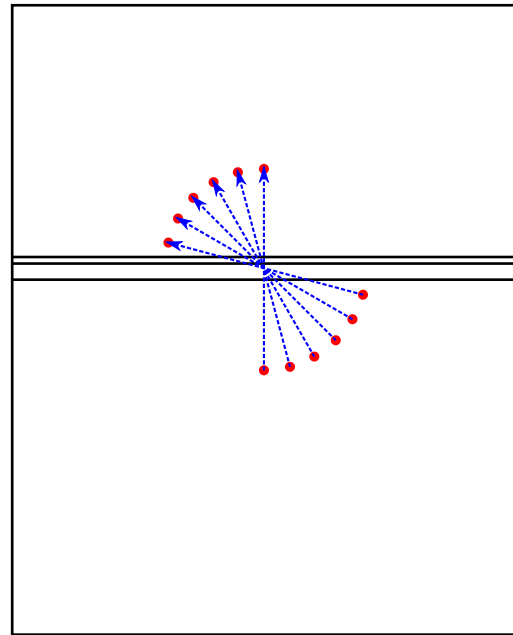
Figure 1: Cross section of the bolted L-section.



Figure 2: Plan view of transmission experiment. Transducers are red circles and measured ray paths are blue dotted arrows.

for a larger feature.

## 4.1 Experimental measurement

A 3 mm thick aluminium L-section was attached to a 3 mm aluminium plate. The L-section was 38 mm in width and height and was attached to the plate with 5 mm diameter bolts which had a 25 mm spacing between them. The bolts were tightened to a torque of 5 N m. The cross section of this structure is shown in figure 1.

12 PZT disk transducers were bonded to the plate in an arc. The transducers were 20 mm in diameter and 1 mm thick. The transducers were bonded with epoxy resin and were held in place by a vacuum bag during bonding. The spacing between the transducers was 40 cm and the transducers were arranged in 2 arcs either side of the L-section, centred in the centre of the L-section which corresponded to a position of a bolt. The angular spacing between the transducers was 15°. The layout of the transducers is shown in figure 2.

The arrangement of the transducers allowed the direct wave paths across the stringer at different incident angles to be collected. The transducers on the lower half of the plate were excited in turn and the ultrasonic wave was measured on the corresponding transducer on the opposite side. The excitation used was a wideband chirp signal from 50 to 500 kHz. From this the responses for 5 cycle toneburst excitations at different frequencies could be deconvolved [19]. The transducers were bonded in place prior to any holes being drilled in the plate to attach the L-section which allowed clear path signals to be collected. Further measurements were then taken after holes had been drilled and then the L-section had been attached. This enables the transmission coefficient of a row of holes and the L-section to be measured.

The transmission coefficient was measured for the first arrival which is the direct path signal between the transducers. In the frequency range considered, the modes are the fundamental symmetric and antisymmetric modes, $A_0$ and $S_0$. In this frequency region the group velocity
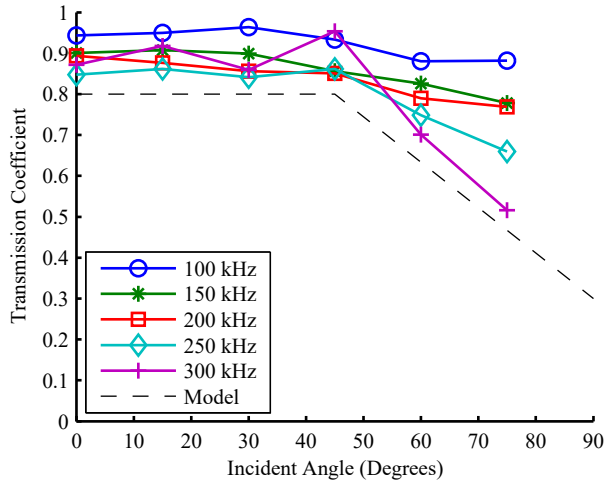
4

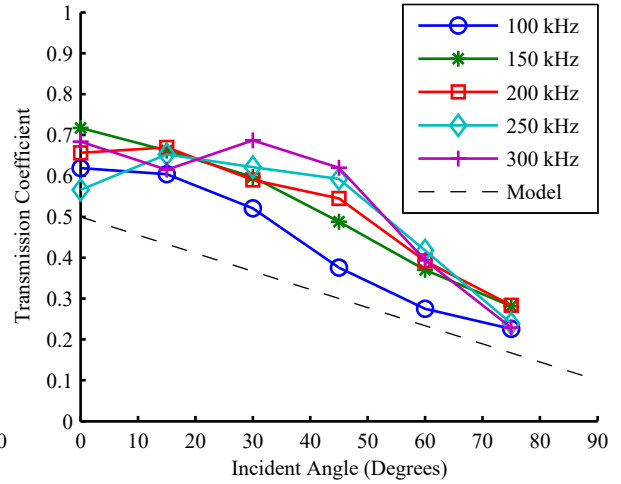Figure 3: The transmission coefficient across a row holes with a 25 mm spacing for different frequencies.



Figure 4: The transmission coefficient across a bolted L-section for different frequencies.

of $S_0$ is always higher so it was for this mode the transmission coefficient was measured. The transmission coefficient was calculated for each frequency as the ratio of maximum amplitude of the envelope of the first arrival between the clear path signal and the feature transmission signal:

$$T = \frac{A_F}{A_C} \tag{2}$$

Where $T$ is the transmission coefficient, $A_F$ is maximum amplitude of the envelope of the feature path first arrival and $A_C$ is the maximum amplitude of the envelope of the clear path first arrival.

Figure 3 shows the experimentally measured transmission coefficient for incident angles of 0° to 75°. For 0° to 45° the transmission coefficient stays constant and is greater than 0.8 for all frequencies. There is only a small difference in transmission for different frequencies with 100 kHz giving the highest value of transmission. At incident angles greater than 45° the behaviour is more frequency dependent with the transmission for higher frequencies being less. The wavelength of the higher frequency waves is more similar to the hole pitch and hole size therefore it is to be expected that the row of holes has a greater affect on these waves. The wavelengths corresponding to the frequencies of interest are shown in table 1 for reference. The transmission for all frequencies decreases to a greater or lesser extent at these incident angles.

The experimentally measured transmission across the L-section is shown in figure 4. In this case the behaviour is similar for all frequencies with the transmission decreasing from a value of about 0.65 to about 0.3 as the incident angle increases. Generally the value of transmission coefficient increases with frequency but the behaviour in this case is less frequency dependant than for the row of holes.

## 4.2 Selection of empirical model

To generalise the uses of this modelling it is desirable to simplify the transmission coefficient models. This is to enable it to be applied to multiple similar features because it would be infeasible to model or experimentally measure transmission across every individual feature in a real aircraft. It is also useful to generalise across different frequencies because the frequency

5

| Frequency (kHz) | Wavelength (mm) |
| --- | --- |
| 100 | 55 |
| 150 | 36 |
| 200 | 27 |
| 250 | 25 |
| 300 | 18 |

Table 1: The wavelengths of the $S_0$ mode in 3 mm aluminium for the frequencies of interest.

| | Position (m) | |
| --- | --- | --- |
| Transducer No. | X | Y |
| 1 | 0.210 | 0.206 |
| 2 | 0.792 | 0.250 |
| 3 | 0.809 | 1.004 |
| 4 | 0.220 | 0.996 |
| 5 | 0.499 | 0.198 |
| 6 | 0.503 | 1.010 |
| 7 | 0.499 | 0.398 |
| 8 | 0.503 | 0.810 |

Table 2: The positions of transducers in the modelling examples.

range AE events generate is not always known and could be in a reasonably wide bandwidth.

In the modelling examples shown here a conservative method of determining the transmission has been chosen. At all frequencies and incident angles the model's value of transmission coefficient is lower than that experimentally measured. This has been done because the most important behaviour of an AE system is that it detects AE events. It would therefore be dangerous if the model suggested that AE events could be detected in regions where that is not the case. It is therefore preferable that the model under predicts on amplitude. The chosen models for a row of holes and a L-section are shown in figures 3 and 4 respectively as dotted lines.

## 5 EXAMPLE USES OF MODELLING

The aim behind the modelling is provide a flexible tool to aid understanding of how an AE system will perform. This can be used to design new experiments or installations or to provide more information about existing setups. Examples of the modelling will now be shown on a $1\,\text{m} \times 1.2\,\text{m}$, 3 mm thick plate with a feature positioned centrally across the plate. Transducers are placed in the positions shown in table 2. The transducers have been deliberately arranged with a small perturbation of up to 5 cm from a geometric grid because this has been found to improve performance of some AE location algorithms by reducing identical triggering times of transducers.

### 5.1 Predicting the triggered transducers

The most important factor in an AE system is that it can detect AE events in the area it is monitoring. An AE event is detected on a transducer if the maximum amplitude of the signal exceeds a threshold. The threshold in this work is 0.01 V which is the estimated maximum amplitude of the noise from [10]. Figures 5 and 6 show the number of transducers that will be triggered by events throughout the plate for 2 different features.

Figure 5 shows the result for a plate with a line of holes feature. This uses the model described in section 4.2. It can been seen that AE events at positions throughout the plate would trigger all 4 transducers and therefore can easily be detected. Figure 6 shows the results in the case where the feature is a bolted L-section. Again the model from section 4.2 has been used. The L-section has a lower transmission coefficient than the line of holes and this means at positions at the sides of the plate the AE events are only detected by 3 transducers. In the central section all transducers can still detect the AE event. AE events can therefore still be
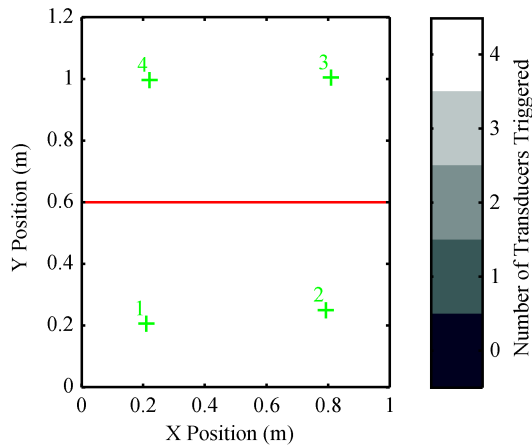
6

Figure 5: The number of transducers (green crosses) AE events at different positions will trigger with row of holes (red line) in between. Each pixel in the image represents an AE source location.
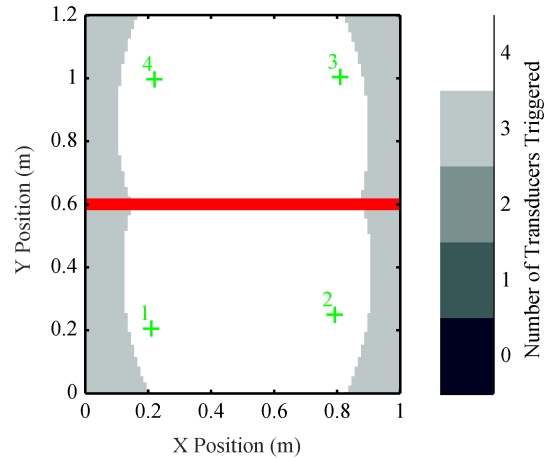
Figure 6: The number of transducers (green crosses) AE events at different positions will trigger with a bolted L-section (red line) in between. Each pixel in the image represents an AE source location.

easily detected throughout the plate.

The number of triggered transducers also determines if and how well AE events can be located. The majority of location methods require at least 3 transducers to be triggered to successfully locate an event. In some cases, as discussed below, it is desirable to use 4 transducers for location and this would not be possible in certain regions of the plate with a bolted L-section.

Given many industrial AE tests are designed just considering the plate properties, where detection limits will be determined by attenuation and beam spread, situations can be conceived where this modelling approach would be useful to guarantee detection and location would be possible.

## 5.2 The influence of number of transducers on location accuracy

In this section the influence on the number of transducers on location performance will be investigated. The location algorithm used will be the Point Method described in [5]. This is a numerical method where an array of $\Delta T$ values, the time difference between triggering of different transducers, are generated for a structure and transducer layout. The closest match in this array to experimentally measured or, in this case, simulated $\Delta T$ values is then found and the location of the AE event is inferred. This method has been chosen in preference to alternative analytical approaches because it is very robust and has been found to perform better in situations with low amplitude signals which is the case here. The $\Delta T$ array has been generated with the plate properties and does not consider the existence of a feature. It would be possible to include this information in the $\Delta T$ array if sufficient information was know about the AE source but as this is often not the case this has not been done.

The structure upon which the location performance will be assessed is the same as the L-section structure in section 5.1 but with two additional transducers to ensure that at least 4 transducers will be triggered by each AE event. That this is the case is shown in figure 7.

The minimum number of transducers required to determine the location of an AE event is 3. This gives 2 $\Delta T$ values to be matched. The location results where 3 transducers are arranged
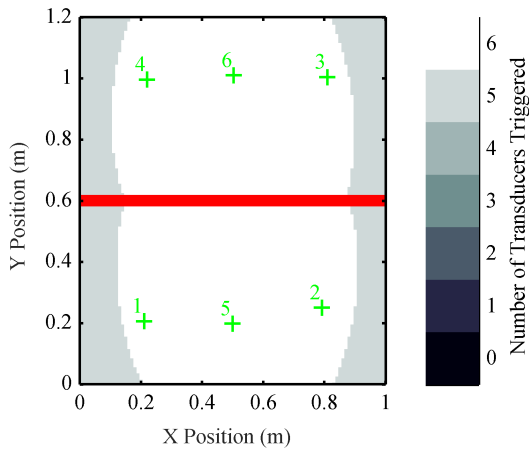
Figure 7: The number of transducers (green crosses) AE events at different positions will trigger with a bolted L-section (red line) in between. Each pixel in the image represents an AE source location.
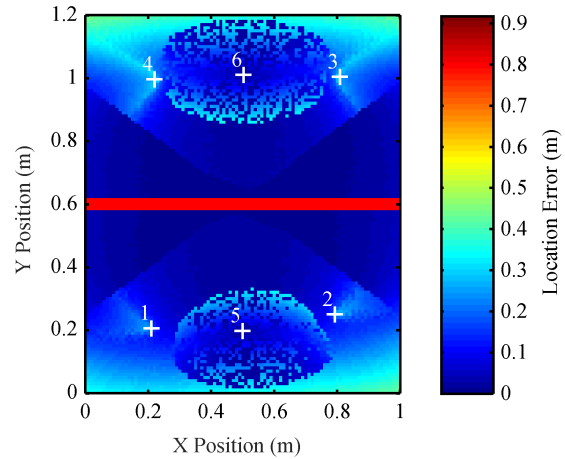


Figure 8: The location error for AE events for a plate with a bolted L-section in the centre (red line). The location algorithm is the point method using 3 transducers. Each pixel in the image represents an AE source location. The transducer locations are show by white crosses.

in approximately a line either side of the feature are shown in figure 8. It can be seen that the location error is generally small but there are regions where the location error is greater than 0.3 m. This includes regions inside the area covered by the transducers. The cause of this error is overlap in the $\Delta T$ array where similar combinations of $\Delta T$ values correspond to markedly different locations. There is a particularly large overlap in this $\Delta T$ array because of the arrangement of the transducers. For many of the AE events in this structure the first 3 triggering transducers will be in a straight line. It is therefore hard for the algorithm to discriminate if this event occurred above or below the line of transducers. This is a well known problem with AE location algorithms and is typically prevented by arranging the transducers in a pattern where they form less shallow triangles. This has been attempted in figure 9. It can be seen that generally the location error is smaller throughout the plate but larger location errors of up to 0.9 m are present in regions surrounding the central transducers. This is again caused by overlap in the $\Delta T$ array. In practise it is very difficult to remove all regions of overlap in the $\Delta T$ array when using only 3 transducers.

Another method of solving this problem is to do location with 4 transducers and therefore 3 $\Delta T$ values. This has been done with the original transducer layout and the result is shown in figure 10. The location error is generally smaller in this example but errors of up to 0.35 m do exist in regions close to the corners of the plate.

This section shows the challenges of arranging transducers to give good location accuracy. This is on simulated data so additional experimental error is likely to exacerbate these challenges. In situations such as this where the signal to noise ratio is low it would be best to tailor the transducer layout to the area where AE is most likely to occur.

## 6 CONCLUSIONS

A modelling approach has been developed to predict the performance of AE systems on structures containing features common in aircraft structures. The modelling approach has low
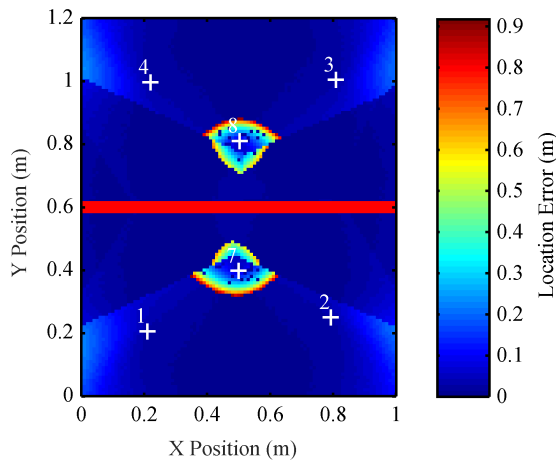
Figure 9: The location error for AE events for a plate with a bolted L-section in the centre (red line). The location algorithm is the point method using 3 transducers. Each pixel in the image represents an AE source location. The transducer locations are show by white crosses.
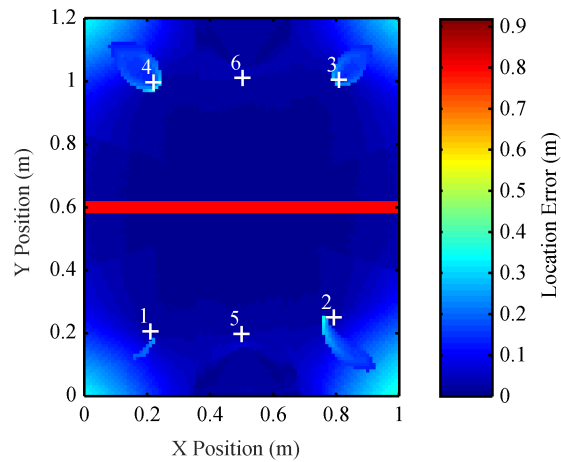
Figure 10: The location error for AE events for a plate with a bolted L-section in the centre (red line). The location algorithm is the point method using 4 transducers. Each pixel in the image represents an AE source location. The transducer locations are show by white crosses.

computational requirements so can be run multiple times to assess how the system will perform for AE events from a large range of locations. The transmission of $S_0$ guided waves across a row of holes and a bolted L-section have been calculated for a variety of incident angles and frequencies and from this empirical models have been created. Uses of the model have then been demonstrated for determining which transducers AE events at different locations will trigger and how the transducer arrangement and number of transducers affects location performance.

The next step in this work is to apply this modelling approach, the feature models described here and feature models from the literature to a section of A320 wing skin which contains thickness changes and L-section like stringers.

## ACKNOWLEDGEMENTS

## REFERENCES

[1] R. Dalton, P Cawley, and M. Lowe, Propagation of acoustic emission signals in metallic fuselage structure. *Science, Measurement and Technology, IEE Proceedings-*, **148**, 169–177, 2001.

[2] E. B. Flynn et al., Enhanced detection through low-order stochastic modeling for guided-wave structural health monitoring. *Structural Health Monitoring*, 1475921711414232, 2011.

[3] A Tobias, Acoustic-emission source location in two dimensions by an array of three sensors. *Non-destructive testing*, **9**, 9–12, 1976.

[4]   C. Paget, K Atherton, and E O'Brien, Triangulation algorithm for damage location in aeronautical composite structures. *Proceedings of the 8th International Workshop on Structural Health Monitoring*, 363–370, 2003.

[5]   J. J. Scholey et al., A generic technique for acoustic emission source location. *Journal of Acoustic Emission*, **27**, 291–298, 2009.

[6]   M. G. Baxter et al., Delta T source location for acoustic emission. *Mechanical systems and signal processing*, **21**, 1512–1520, 2007.

[7]   M. A. Hamstad, A review: acoustic emission, a tool for composite-materials studies. *Experimental Mechanics*, **26**, 7–13, 1986.

[8]   J. J. Scholey et al., Quantitative experimental measurements of matrix cracking and delamination using acoustic emission. *Composites Part A: Applied Science and Manufacturing*, **41**, 612–623, 2010.

[9]   J. J. Scholey, The development of a quantitative framework for acoustic emission testing. PhD thesis, University of Bristol, 2008.

[10]  C. K. Lee et al., Acoustic emission during fatigue crack growth in aluminium plates. *9th European Conference on Nondestructive Testing*, 2006.

[11]  V. Pagneux and A. Maurel, Lamb wave propagation in elastic waveguides with variable thickness. *Proceedings of the Royal Society A: Mathematical, Physical and Engineering Science*, **462**, 1315–1339, 2006.

[12]  Y. Cho, Estimation of ultrasonic guided wave mode conversion in a plate with thickness variation. *Ultrasonics, Ferroelectrics and Frequency Control, IEEE Transactions on*, **47**, 591–603, 2000.

[13]  S. Rokhlin, Lamb wave interaction with lap-shear adhesive joints: Theory and experiment. *The Journal of the Acoustical Society of America*, **89**, 2758–2765, 1991.

[14]  P. B. Nagy and L. Adler, Nondestructive evaluation of adhesive joints by guided waves. *Journal of Applied Physics*, **66**, 4658–4663, 1989.

[15]  M. Lowe, R. Challis, and C. Chan, The transmission of Lamb waves across adhesively bonded lap joints. *The Journal of the Acoustical Society of America*, **107**, 1333–1345, 2000.

[16]  R. Dalton, P Cawley, and M. Lowe, The potential of guided waves for monitoring large areas of metallic aircraft fuselage structure. *Journal of Nondestructive Evaluation*, **20**, 29–46, 2001.

[17]  Y. Liu et al., Structural health monitoring and damage detection in composite panels with multiple stiffeners. *Proceedings of 52nd AIAA/ASME/ASCE/AHS/ASC Structures, Structural Dynamics, and Materials Conference*, 2011.

[18]  J. J. Scholey and P. D. Wilcox, *Acoustic Emission for the Localization of Damaged Regions in Structures as Part of the NDE Process*, tech. rep., RCNDE Targeted Research Project, 2007.

[19]  J. E. Michaels et al., Chirp excitation of ultrasonic guided waves. *Ultrasonics*, **53**, 265–270, 2013.